International Conference on Mathematics and Computational Methods Applied to Nuclear Science and Engineering (M&C 2011)
Rio de Janeiro, RJ, Brazil, May 8-12, 2011, on CD-ROM, Latin American Section (LAS) / American Nuclear Society (ANS)
ISBN 978-85-63688-00-2

A GENERAL COARSE AND FINE MESH SOLUTION SCHEME FOR FLUID FLOW MODELING IN VHTRS

Clifford I, Ivanov K and Avramova M
The Pennsylvania State University
334 Reber Building, University Park, PA 16802, USA
ivor.clifford@psu.edu; kni1@psu.edu; mna109@psu.edu

ABSTRACT

Coarse mesh Computational Fluid Dynamics (CFD) methods offer several advantages over traditional coarse mesh methods for the safety analysis of helium-cooled graphite-moderated Very High Temperature Reactors (VHTRs). This relatively new approach opens up the possibility for system-wide calculations to be carried out using a consistent set of field equations throughout the calculation, and subsequently the possibility for hybrid coarse/fine mesh or hierarchical multi-scale CFD simulations. To date, a consistent methodology for hierarchical multi-scale CFD has not been developed. This paper describes work carried out in the initial development of a multi-scale CFD solver intended to be used for the safety analysis of VHTRs. The VHTR is considered on any scale to consist of a homogenized two-phase mixture of fluid and stationary solid material of varying void fraction. A consistent set of conservation equations was selected such that they reduce to the single-phase conservation equations for the case where void fraction is unity. The discretisation of the conservation equations uses a new pressure interpolation scheme capable of capturing the discontinuity in pressure across relatively large changes in void fraction. Based on this, a test solver was developed which supports fully unstructured meshes for three-dimensional time-dependent compressible flow problems, including buoyancy effects. For typical VHTR flow phenomena the new solver shows promise as an effective candidate for predicting the flow behavior on multiple scales, as it is capable of modeling both fine mesh single phase flows as well as coarse mesh flows in homogenized regions containing both fluid and solid materials.

Key Words: VHTR, thermal-fluids, multi-scale, coarse mesh CFD

1. INTRODUCTION

Evaluations of fluid behavior and heat transfer phenomena in helium-cooled, graphite-moderated, very high temperature reactors (VHTRs) at normal operational conditions and during abnormal or accident conditions are critical to ensuring the safety of designs and it is in this area where many of these uncertainties are to be found. The traditional approach for full core analysis has been to use coarse mesh methods customized to the particular problem at hand. For HTRs a porous medium approach is most common. However, the methodology for deriving effective homogenized flow and heat transfer parameters is not well established. The traditional coarse mesh approaches are therefore unable to provide solutions with sufficient accuracy and detail to address these uncertainties.

The availability of high-resolution computational fluid dynamics (CFD) has opened up the possibility to model the fluid flow and heat transfer within regions of the reactor in high detail. The great appeal of the CFD codes is their reliance on first principles to describe the fluid

behavior and their capability to calculate the behavior of many complex flow patterns. For HTRs, where the coolant is a single-phase gas, CFD methods are particularly suitable. At present, however, the computational resources required for full core CFD analysis are prohibitively large, making them unsuitable for day-to-day safety analysis.

It is possible, however, to use coarse mesh CFD methods, which provide a number of advantages. The primary advantage is that system-wide calculations can be carried out using a consistent set of field equations throughout the calculation. This opens up the possibility for hybrid coarse/fine mesh or hierarchical multi-scale CFD simulations, where the detailed fine mesh solution is homogenized to determine consistent coarse mesh parameters and subsequently improve the accuracy of the coarse mesh solution. To date, however, a consistent methodology for hierarchical multi-scale CFD has not been developed [1].

In this work, we introduce a coarse mesh CFD solution scheme applicable for multi-scale CFD simulation of VHTRs, with the intent of applying this for future developments and research into hierarchical multi-scale CFD simulations of this reactor type. In Section 2 we present a generalized description of the helium-cooled graphite-moderated VHTR from a thermal-fluids perspective. Based on this description, a consistent set of modeling equations based on the two-phase continuous medium flow equations is presented in Section 3. Issues surrounding the numerical discretisation and solution of the modeling equations are discussed in Section 4. The solver implementation is described in Section 5. Section 6 presents some initial results and further discussion regarding the accuracy and stability of the developed solver. Conclusions and recommendations for future work are given in Section 7.

2. GENERALIZED DESCRIPTION OF A VHTR FROM A THERMAL-FLUIDS PERSPECTIVE

Current VHTR concepts and designs may be separated into two distinct design types, namely the pebble bed and prismatic VHTRs. The pebble bed design employs fuel in the form of graphite spheres, which are dropped into and continuously circulated through a cylindrical or annular core using online refueling. The prismatic or block-type design features a core comprised of graphite blocks containing an array of cylindrical fuel compacts with channels bored vertically through the graphite blocks for coolant flow. Despite these basic geometric differences, from a thermal-fluids perspective, both designs are characterized by several common features.

- The coolant is single-phase helium gas.
- The core structures are composed primarily of graphite with steel supporting structures and pressure vessel.
- The geometry of the design exhibits multiple spatial scales; namely the micro (TRISO coated particles), meso (fuel sphere of fuel block) and macro (full core) scales.
- From the macroscopic perspective the reactor unit can be separated into numerous regions, which contain either fluid, solid, or a mixture of fluid and solid components.
- There are numerous heat transferring surfaces between fluid and solid regions.

The current generation of pebble-bed thermal-fluid solvers employ a porous medium flow model within the core and a one-dimensional network approach elsewhere in the reactor pressure

vessel [1,2,3]. The methods employed by the current generation of solvers for the prismatic VHTR may vary but, in general, either a porous medium or one-dimensional network approach is employed within the core, while a one-dimensional network approach is used elsewhere in the reactor pressure vessel [4,5]. In this work, we take the view that the VHTR can be represented on any scale as a two-phase mixture containing a fluid phase and a stationary solid phase with varying porosity. In many respects, this is like the porous medium approximation when considering the macroscopic scale; however, when modeling the microscopic scale, the porosity is unity and this approximation reduces to single-phase flow with surface heat transfer within the fluid containing regions. In terms of geometrical representation we opt for a three-dimensional CFD-type unstructured mesh since this provides the greatest flexibility. One particular advantage of this approach is that unstructured meshes can be generated to include regions that mimic one- and two-dimensional elements, thus allowing us to leverage the advantages of both the one-dimensional network and the porous medium approaches on the macroscopic scale.

3. BASIC MODELING EQUATIONS

The equations employed are derived from the work of Saurel [6,7]. These equations are written for a general two-phase mixture. We simplify these for the case of a two-phase gas and stationary solid mixture, as we would encounter in a typical homogenized model of a VHTR or sub-region thereof. The basic modeling equations are obtained by assuming no mass transfer between the phases and a time-independent void fraction.

$$\frac{\partial \varepsilon \rho_g}{\partial t} + \nabla \cdot \left(\varepsilon \rho_g \vec{u}_g \right) = 0 \tag{1}$$

$$\frac{\partial \varepsilon \rho_g \vec{u}_g}{\partial t} + \nabla \cdot \left(\varepsilon \rho_g \vec{u}_g \otimes \vec{u}_g + \varepsilon P_g \right) + \nabla \cdot \left(\varepsilon \boldsymbol{\tau}_g \right) = P_i \nabla \varepsilon + \vec{F}_{dg} + \varepsilon \rho_g \vec{g} \tag{2}$$

$$\frac{\partial \varepsilon \rho_g E_g}{\partial t} + \nabla \cdot \left(\vec{u}_g \left(\varepsilon \rho_g E_g + \varepsilon P_g \right) \right) + \nabla \cdot \vec{q}_g'' = \left(\vec{F}_{dg} + \rho_g \vec{g} \right) \cdot \vec{u}_i + Q_g''' \tag{3}$$

$$\frac{\partial (1-\varepsilon) \rho_s h_s}{\partial t} + \nabla \cdot q_s'' = Q_s''' \tag{4}$$

Here ε is the porosity of the mixture. ρ, $\vec{u}$, E and h are the density, velocity, total energy $\left(E \equiv e + \frac{1}{2} \left| \vec{u} \right|^2 \right)$ and enthalpy respectively. $\vec{F}_d$ is the inter-phase drag term and q'' is the conductive heat flux. Q''' is the heat source, which includes the inter-phase heat transfer term. The subscripts g and s denote the gas and solid phases respectively. The gravitational term has also been included in the momentum and energy equations.

In equations (2) and (3), P_i and $\vec{u}_i$ are the average interfacial pressure and velocity respectively. In most references, $\vec{u}_i$ and P_i are assumed equal to those for the incompressible or the less compressible phase [6], in our case the solid phase. For $\vec{u}_i$, however, we choose $\vec{u}_i \equiv \vec{u}_g$ to ensure that the energy equation yields the single-phase energy equation as $\varepsilon \to 1$.

$$\vec{u}_i \equiv \vec{u}_g \tag{5}$$

$$P_i \equiv P_s = P_g + \tfrac{1}{2}\rho_g \left|\vec{u}_g\right|^2 \tag{6}$$

The inter-phase drag term is written in terms of a nonlinear tensor drag coefficient $\boldsymbol{\kappa}(\vec{u}_g)$. This may be compared to the traditional Darcy porous drag term. In this case, however, we allow for the possibility that the drag is anisotropic in nature.

$$\vec{F}_{dg} = \varepsilon \boldsymbol{\kappa}(\vec{u}_g) \cdot \vec{u}_g \tag{7}$$

In the equations of Saurel [6,7] the momentum and thermal diffusion terms are absent since they are not easily defined for multi-phase flows. While this assumption may be valid for flows where inter-phase drag and heat transfer effects dominate, for the case of $\varepsilon = 1$ we expect the equations to reduce to the single phase flow equations, where these terms are typically included. We have therefore reintroduced these terms in the two-phase conservation equations, noting that suitable models must be defined in order to treat these terms for the case of $\varepsilon \neq 1$.

In equation (2), $\boldsymbol{\tau}$ is the stress tensor, which has been included to account for momentum diffusion, turbulent mixing and dispersion effects. Numerous methods are available for evaluating this term for single-phase flows, including the standard Reynold's Averaged Navier-Stokes (RANS) and Large Eddy Simulation (LES) methods accompanied by a suitable turbulence model such as the well-known $k-\varepsilon$ model. These models are used to define effective turbulent viscosity and thermal diffusivity values to be used in the single-phase Navier-Stokes equations. General-purpose turbulence models such as $k-\varepsilon$ and $k-\Omega$ assume a clear fluid and that the generation of turbulence is dependent only on the macroscopic flow variables and macroscopic geometry. These traditional turbulence models are not directly applicable to heterogeneous mixtures of fluid and solid phases on the fine scale. However, a certain amount of research has been directed towards describing the turbulent behavior of a fluid flow in the presence of a solid phase, which may or may not be periodic in nature. As examples, the work of Pedras and de Lemos [8] as well as Chandesris et al. [9] yield modified forms of the $k-\varepsilon$ turbulence model that include additional terms for the dispersion effects of the solid phase. For the purposes of this work, we do not consider these models in detail. This is reserved for future work. In the current context, it is sufficient to note that the RANS approach, along with the standard $k-\varepsilon$ turbulence model, is applicable if suitable modifications are applied to the $k-\varepsilon$ turbulence model in the two-phase regions.

A final modification is made in order to improve the numerical precision of the pressure solution, by defining the pressure in terms of a specified reference or gauge pressure. We define the pressure as the sum of the reference pressure P_0 and a pressure variation δP.

$$P_g = P_{ref} + \delta P_g \tag{8}$$

This is substituted into the momentum equation. The final set of modeling equations for the gas phase becomes the following.

$$\frac{\partial \varepsilon \rho_g}{\partial t} + \nabla \cdot \left(\varepsilon \rho_g \vec{u}_g \right) = 0 \tag{9}$$

$$\frac{\partial \varepsilon \rho_g \vec{u}_g}{\partial t} + \nabla \cdot \left(\varepsilon \rho_g \vec{u}_g \otimes \vec{u}_g \right) + \nabla \cdot \left(\varepsilon \boldsymbol{\tau}_g \right) = -\varepsilon \nabla \delta P_g + \rho_g K_g \nabla \varepsilon + \varepsilon \boldsymbol{\kappa} \cdot \vec{u}_g + \varepsilon \rho_g \vec{g} \tag{10}$$

$$\frac{\partial \varepsilon \rho_g E_g}{\partial t} + \nabla \cdot \left(\vec{u}_g \left(\varepsilon \rho_g E_g + \varepsilon P_g \right) \right) + \nabla \cdot \vec{q}_g'' = \left(\varepsilon \boldsymbol{\kappa} \cdot \vec{u}_g + \varepsilon \rho_g \vec{g} \right) \cdot \vec{u}_g + Q_g''' \tag{11}$$

It is convenient for us to rewrite the energy equation (11) in terms of total enthalpy $\left(H \equiv E + \rho^{-1} P \right)$ or enthalpy $\left(h \equiv e + \rho^{-1} P \right)$ largely because this allows us to write the heat conduction term in terms of the thermal diffusivity $\left(\alpha \equiv {c_P}^{-1} k \right)$. This is important for turbulence modeling since here we relate the turbulent thermal diffusivity to the turbulent viscosity through the Prandtl number. Written in terms of total enthalpy and enthalpy, the energy equation takes on the following forms.

$$\frac{\partial \varepsilon \rho_g H_g}{\partial t} + \nabla \cdot \left(\varepsilon \rho_g \vec{u}_g H_g \right) + \nabla \cdot \vec{q}_g'' = \frac{\partial \varepsilon P_g}{\partial t} + \left(\varepsilon \boldsymbol{\kappa} \cdot \vec{u}_g + \varepsilon \rho_g \vec{g} \right) \cdot \vec{u}_g + Q_g''' \tag{12}$$

$$\frac{\partial \varepsilon \rho_g h_g}{\partial t} + \nabla \cdot \left(\varepsilon \rho_g h_g \vec{u}_g \right) + \nabla \cdot \vec{q}_g'' = \frac{\partial \varepsilon P_g}{\partial t} + \varepsilon \vec{u}_g \cdot \nabla P_g + \nabla \cdot \left(\varepsilon \boldsymbol{\tau}_g \vec{u}_g \right) - \left(\nabla \cdot \varepsilon \boldsymbol{\tau}_g \right) \cdot \vec{u}_g + Q''' \tag{13}$$

where $\vec{q}_g'' = -\varepsilon \alpha_t \nabla h_g$ and α_t is the turbulent thermal diffusivity.

4. NUMERICAL SOLUTION OF THE BASIC MODELING EQUATIONS

The equations of Section 3 are discretized using the standard finite-volume method on a collocated mesh. While most of the equation terms closely resemble their single phase flow counterparts, special attention is needed for certain terms primarily because of the potential for discontinuities in the void fraction at the interfaces between different regions. Standard Finite Volume discretisation assumes a smooth variation in flow parameters and the discontinuous behavior of the pressure and velocity that occurs at these interfaces leads to unbounded, unstable and unphysical solutions. We will reconsider these issues in later sections and for now introduce a semi-implicit solution scheme that employs a Pressure Implicit Split Operator (PISO) type of approach for the pressure-velocity coupling.

4.1. The Solution Scheme

The solution scheme employed is a modified form of the scheme suggested by Jasak [12]. The momentum equation (10) is written in a semi-discretized form as below.

$$A_P \vec{u}_g = \vec{H}\left(\vec{u}_g \right) - \varepsilon \nabla \delta P_g$$

Here A_P contains the diagonal terms from the momentum equation solution matrix and $\vec{H}(\vec{u}_g)$ comprises the off-diagonal terms and source term contributions. From this the velocity is expressed as follows.

$$\vec{u}_g = \frac{1}{A_P}\left[\vec{H}(\vec{u}_g) - \varepsilon \nabla \delta P_g\right] \tag{14}$$

From this we may express the mass flux $\vec{\phi}$ in terms of pressure as follows.

$$\vec{\phi}_g \equiv \varepsilon \rho_g \vec{u}_g = C\left(\vec{K} - \nabla \delta P\right) \tag{15}$$

Here the linearized coefficients C and K are defined as below.

$$C \equiv \frac{\varepsilon^2 \rho_g}{A_P} \tag{16}$$

$$\vec{K} \equiv \frac{\vec{H}(\vec{u}_g)}{\varepsilon} \tag{17}$$

We next substitute (15) into the mass conservation equation (9) and use the equation of state to rewrite the time-derivative of density in terms of pressure. The resulting pressure correction equation becomes the following.

$$\frac{\partial \varepsilon \psi_g \delta P_g}{\partial t} + P_{ref} \frac{\partial \varepsilon \psi_g}{\partial t} - \nabla \cdot C \nabla \delta P_g + \nabla \cdot C\vec{K} = 0 \tag{18}$$

Here ψ_g is the fluid compressibility (ρ / P) derived from the fluid equation of state.

The final solution algorithm is as follows:

1. Start of time step.
2. Solve the mass conservation equation (9) using most recent mass flux values to yield predicted density values.
3. Solve the momentum equation (10) using the most recent pressure, density values and mass flux values to yield predicted velocities.
4. Solve the energy equation (12) or (13).
5. Use the equation of state to correct the density as a function of pressure and temperature.
6. Solve the pressure correction equation (18) yielding corrected pressures.
7. Correct the mass fluxes using equation (15).
8. Solve the mass conservation equation (9) to yield corrected density values.
9. Correct the velocities using equation (14).
10. Repeat steps 4 through 9 until the desired convergence is achieved.
11. End of time step.

4.2. Issues of Discretization

The treatments for several discretisation issues are based on the work of du Toit [11]. In our case, however, the approach has been generalized for three-dimensional unstructured meshes and a number of additional modifications have been introduced.

4.2.1. Momentum interpolation

The evaluation of the divergence term in the mass conservation equation (9) requires an expression for the mass flux at the cell faces. For this, we consider equation (15). The inherent problem with this expression is that it applies for the cell center and we do not know how to determine C and $\vec{K}$ at the faces. We opt to use a similar approach to that in typical conjugate heat transfer problems; we equate the mass flux at the face *(f)* from both the owner *(P)* and neighbour *(N)* cells as defined in Figure 1.

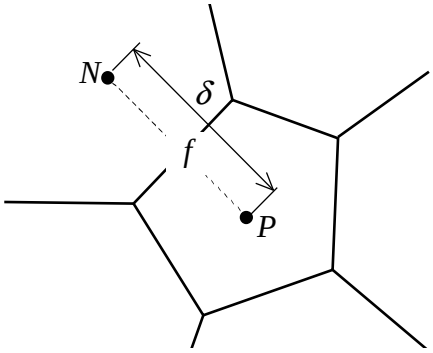

Figure 1. Control Volume Definition for a Typical Finite-Volume Discretization

$$\vec{\phi}_f = \vec{\phi}_{fP} = \vec{\phi}_{fN}$$
$$C_f\left(\left(\nabla \delta P\right)_f - \vec{K}_f\right) = C_P\left(\left(\nabla \delta P\right)_{fP} - \vec{K}_P\right) = C_N\left(\left(\nabla \delta P\right)_{fN} - \vec{K}_N\right)$$

Applying a finite differencing across the cell face, we yield the following expressions for the linearized coefficients and pressure at the cell face after some manipulation.

$$C_f = \frac{C_N C_P}{\beta_f C_P + \left(1-\beta_f\right)C_N} \tag{19}$$

$$\vec{K}_f = \left(1-\beta_f\right)\vec{K}_P + \beta_f \vec{K}_N \tag{20}$$

$$\delta P_f = \frac{\beta_f C_P \delta P_P + \left(1-\beta_f\right)C_N \delta P_N}{\beta_f C_P + \left(1-\beta_f\right)C_N} + \frac{\beta_f\left(1-\beta_f\right)\delta_f{}^2}{\beta_f C_P + \left(1-\beta_f\right)C_N}\frac{C_P\vec{K}_P - C_N\vec{K}_N}{\delta_f} \tag{21}$$

Here β_f is a face interpolation parameter $\left(0 \le \beta_f \le 1\right)$ and δ_f is the distance between cell centers for the cells *P* and *N*. Equation (19) represents harmonic interpolation of the coefficient C as would typically be seen in conjugate heat transfer problems. Equation (20) represents reverse linear interpolation. Equation (21) for the face pressure includes two terms, the first being bounded and the second an extrapolation based on the surface-normal gradient of $C\vec{K}$. We can expect that this extrapolation will be problematic for certain classes of problems. Having noted that this second term is the surface-normal gradient, we may apply typical Finite Volume corrections in the evaluation of this term on non-orthogonal meshes.

4.2.2. The momentum convection term

The momentum convection term is a source of inconsistency since typical discretisation of this term uses upwind or higher order Gudonov-type or similar discretisation schemes for stability reasons. Further the choice of which scheme to employ is typically to the CFD analyst's discretion. This is problematic since the discontinuity in velocity must be matched closely with the pressure and density variations for a stable and consistent solution. Consider Figure 2, which depicts this problem.

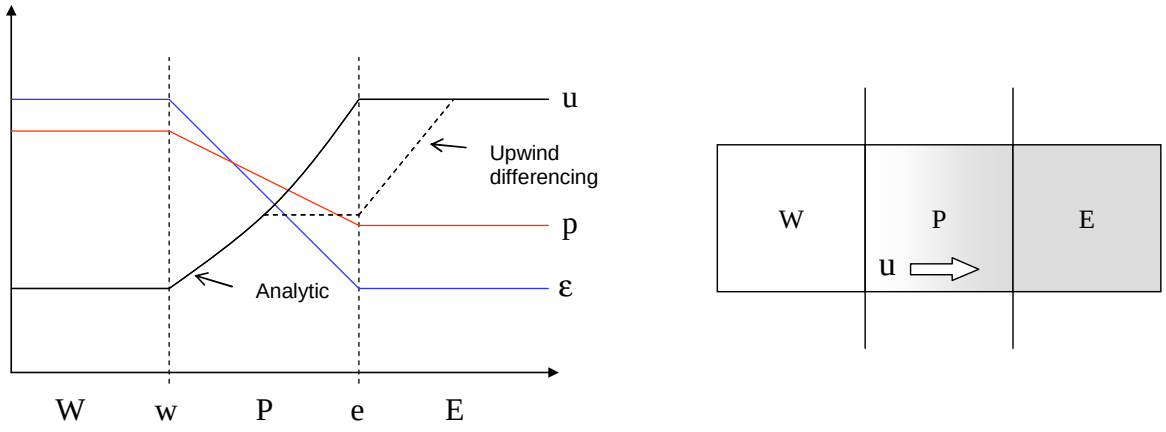

Figure 2. The Change in Flow Parameters at a Porosity Jump

We note, however, that although the velocity may be discontinuous across the interface, the mass flux is not. We can therefore modify the convection term as follows.

$$\nabla \cdot \vec{\phi}_g \otimes \bar{u}_g \Rightarrow \nabla \cdot \left(\frac{\vec{\phi}_g}{\varepsilon \rho_g} \otimes \varepsilon \rho_g \bar{u}_g \right) \tag{22}$$

Here the left hand term in the cross product is evaluated explicitly forming a linear operator in terms of velocity. By applying the user-selected velocity interpolation scheme to $\varepsilon \rho_g \bar{u}_g$, the

discontinuity in porosity is treated consistently in a conservative manner. It is also possible to apply the interpolation to the superficial velocity $\varepsilon \vec{u}_g$ but initial tests suggest that the inclusion of density is helpful in treating some of the unboundedness associated with equation (21). While the mass flux at the face is known from equations (15), (19) and (20), an expression for $\varepsilon\rho_g$ at the face is absent. We define this by noting that, for a linear variation in velocity with constant mass flux, a linear variation in $(\varepsilon\rho_g)^{-1}$ is required. We therefore apply linear interpolation to $(\varepsilon\rho_g)^{-1}$.

4.2.3. Time step dependence of the solution

For time-dependent problems on collocated grids the presence of the time step Δt in the linearized coefficients C and $\vec{K}$, which are then interpolated to the cell faces, generally leads to a time step dependent solution. For the particular interpolation schemes, chosen in equations (19) and (20), it is convenient that the structure of the coefficients is preserved during the interpolation process and we therefore do not expect any problems in this regard. However, the presence of the old time term $\rho_g u_{g0}/\Delta t$ in the coefficient $\vec{K}$ results in a time step dependent solution. By noting that this can be replaced directly with the previous time step mass flux $\vec{\phi}_{g0}/\varepsilon\Delta t$, which is already defined at the cell faces, the solution then becomes time step independent.

5. IMPLEMENTATION

The equations and solution scheme of Section 4 have been implemented using the OpenFOAM multi-physics toolkit [13]. This toolkit provides automatic matrix construction and solution for scalar and vector equations using standard Finite Volume approaches based on user-specified differencing and interpolation schemes. Additional schemes were implemented according to the equations of Section 4 where necessary. The current test solver is a fully unstructured three-dimensional time-dependent compressible flow solver, including gravity, with support for a variable porosity field.

6. INITIAL RESULTS AND DISCUSSION

In this section we present initial results that have been obtained using the test solver of Section 5. We start with relatively simple test calculations to demonstrate the solver performance for relatively large changes in porosity in Section 6.1. The results for some more advanced test calculations have been included in Section 6.2.

6.1. Simple Test Calculations

The first test calculation simulates a simple one-dimensional pipe containing two porous regions with void fractions of 0.1 and 0.01 respectively. The drag coefficient in the each is set to zero in order to capture the change in pressure caused by flow acceleration (Bernoulli effect). The inlet velocity is 1 m/s and standard atmospheric conditions are assumed. Air as an ideal gas is

assumed. The very small void fraction of 0.01 is an extreme example that results in velocities in the order of 100 m/s where compressibility effects are important. Steady-state velocity and pressure profiles are given in Figure 3. The velocity and pressure both behave as expected, however we note small inconsistencies near the discontinuities. In particular, the change in pressure extends over more than one cell length on either side of the discontinuity. The result of this is an overall loss in pressure at the outlet of 57 Pa, 1% of the pressure drop caused by the accelerating flow (6.25 kPa). The inconsistency is not present when the flow is assumed incompressible.

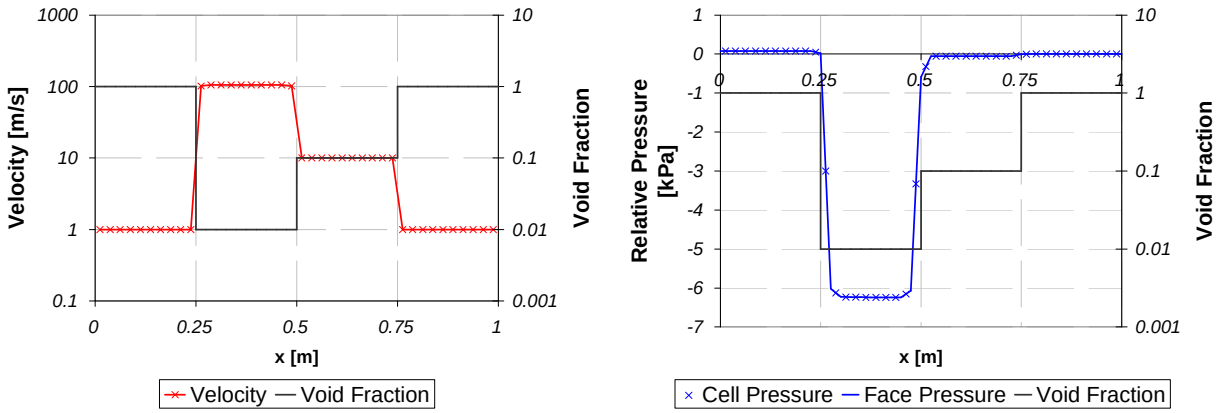

Figure 3. Velocity and Pressure for a One-dimensional Pipe with no Friction and Varying Void Fraction

We next consider a similar case with a single porous region of length 0.5 m and void fraction of 0.05. A drag coefficient of 1×10^{4} Pa.s.m^{-2} is assumed. The expected pressure drop for this problem, using air as an ideal gas and assuming an adiabatic process at constant mass flow rate is 127.5 kPa. This compares well with the value of 127.59 kPa calculated by the solver (0.1% error) and shown in Figure 4. Similarly, the calculated exit temperature of 237.8 K compares well with the analytical value of 237.2 K (1% error). A portion of this error is caused by the relative coarseness of the mesh (40 elements). With a much finer mesh (160 elements), the error in outlet temperature is reduced to 0.5%. Clearly noticeable in this case is the advantage that the pressure interpolation scheme provides at the porous interface. Here the discontinuity in the gradient of pressure is captured well and there is no need to refine the mesh in this region to capture this effect.

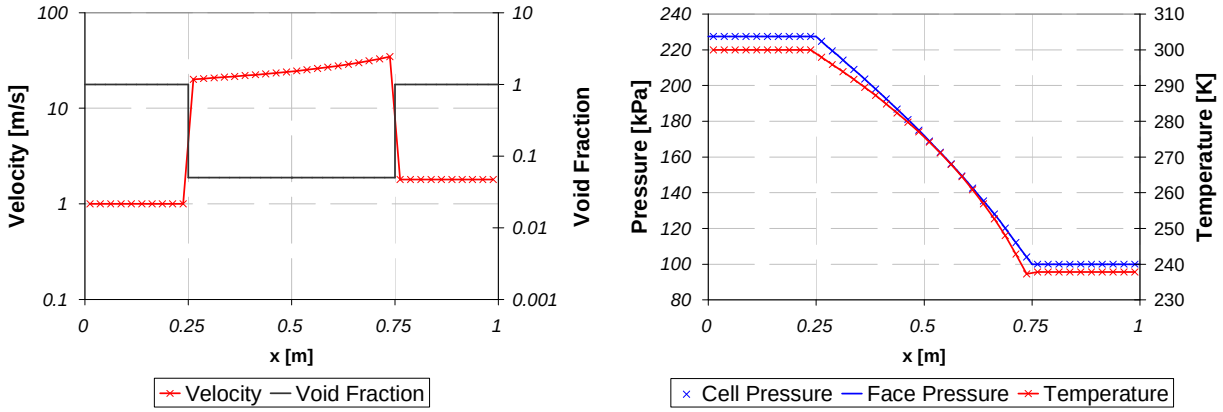

Figure 4. Velocity and Pressure for a One-dimensional Pipe with Varying Void Fraction

A similar problem was calculated for a two-dimensional 90^{o} pipe bend containing a porous region. Here the stability of the solver is demonstrated for a more complex problem. The results for this calculation are in similar agreement to the previous one-dimensional test calculation. For this calculation, the solver is stable within the typical Courant number limit of 0.3.

The final one-dimensional test case demonstrates the unboundedness of the pressure interpolation scheme, which is caused by strong flow discontinuities, in this case a normal shock wave. The void fraction is varied in a smooth fashion to obtain the typical inlet profile of a supersonic wind tunnel. Figure 5 clearly shows how, with increasing simulation time, the flow velocity increases until it exceeds the speed of sound and begins to form a normal shock wave. With the formation of the shock wave the instability in the pressure interpolation scheme is clearly visible as strong oscillations in the face pressures.

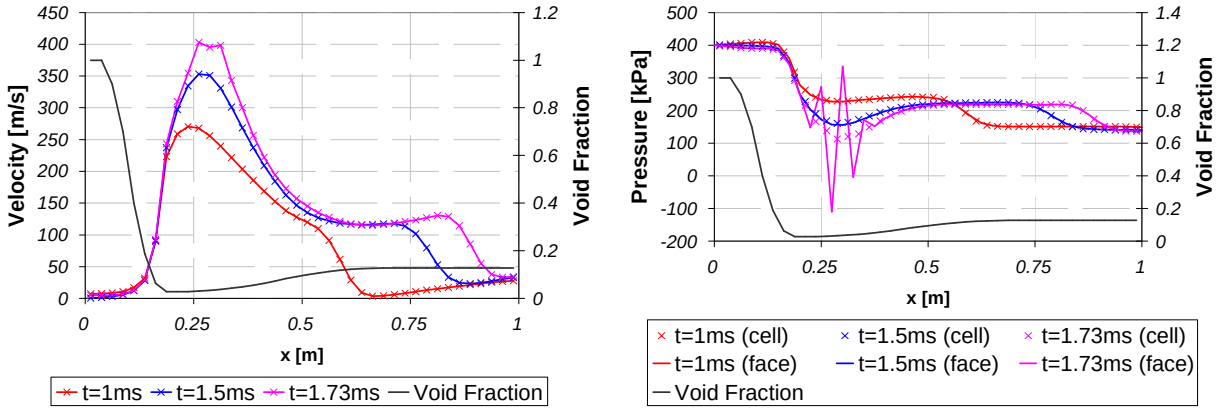

Figure 5. Unboundedness of the Pressure Interpolation Scheme for Shock Problems

An attempt was made to bound the face pressure within the neighboring cell pressures. While this does stabilize the solution, it also influences the solution behavior across discontinuities in void fraction. While it is not likely that we will model such strong phenomena in VHTRs, this could be problematic when modeling accidents such as a depressurized loss of forced cooling (DLOFC) where pressure waves will may be present in the system.

6.2. A Representative Three-Dimensional Test Calculation

In order to demonstrate the applicability of this approach to modeling of VHTRs, a representative three-dimensional model of a prismatic reactor core was developed. Since this is a demonstration calculation, and in order to reduce the development time, a small model was developed comprising only three axial layers of hexagonal fuel elements, each with six fuel elements in an annular arrangement surrounding a hexagonal central reflector block. The fuel dimensions are based on GT-MHR fuel, i.e. 80cm high and 36 cm across the flats with a void fraction of 18%. The fuel elements themselves are modeled as homogenized hexagonal blocks containing 61 one-dimensional flow channels separated by baffles. A coaxial arrangement of the coolant inlet and outlet and pipes is used. Cylindrical plena are located above and below the core. A sinusoidal fuel temperature profile is specified in both radial and axial directions as a heat source to the coolant flow.

The mesh for this model is shown in Figure 6(a). As can be seen, the mesh makes extensive use of polyhedral elements. This was done not only to conform to the hexagonal shape of the fuel but also to avoid the use of triangular elements which often yield poor quality results for finite-volume solvers. The mesh contains a total of 43,000 cells and 192,000 faces. Of the faces, 109,000 are internal faces. On average therefore, each cell has 2.5 neighboring cells. This small number is driven by the large number of one-dimensional elements present.

The current model assumes there are no gaps between the fuel elements since the meshing of these was found to be particularly problematic. With gap widths of between 0.5 and 2mm, direct meshing of the gap regions introduces cells with large aspect ratios. This is not necessarily a problem, for example, midway down the fuel element, since here the flow is two-dimensional in nature and the very small third dimension is perpendicular to the flow direction. The problem is greatest where the gap elements must couple to other mesh elements, for example in the plena. This yields elements with high aspect ratios in these regions where it is undesirable. Refining these mesh elements is also undesirable since this will significantly reduce the allowable time step. A further issue is how to model the horizontal gaps between the top and bottom surfaces of fuel blocks since here the small dimension of the gap aligns with the direction of flow, once again limiting the allowable time step.

Figure 6(b) shows some results obtained for typical steady-state operation. The solver captures the three-dimensional nature of the flow in the void regions, while at the same time capturing the flow behavior through the homogenized fuel elements. Similar calculations were carried out for time-dependent buoyancy driven flows using this model. While yet to be fully verified, the results of these calculations are promising and the solver is stable.

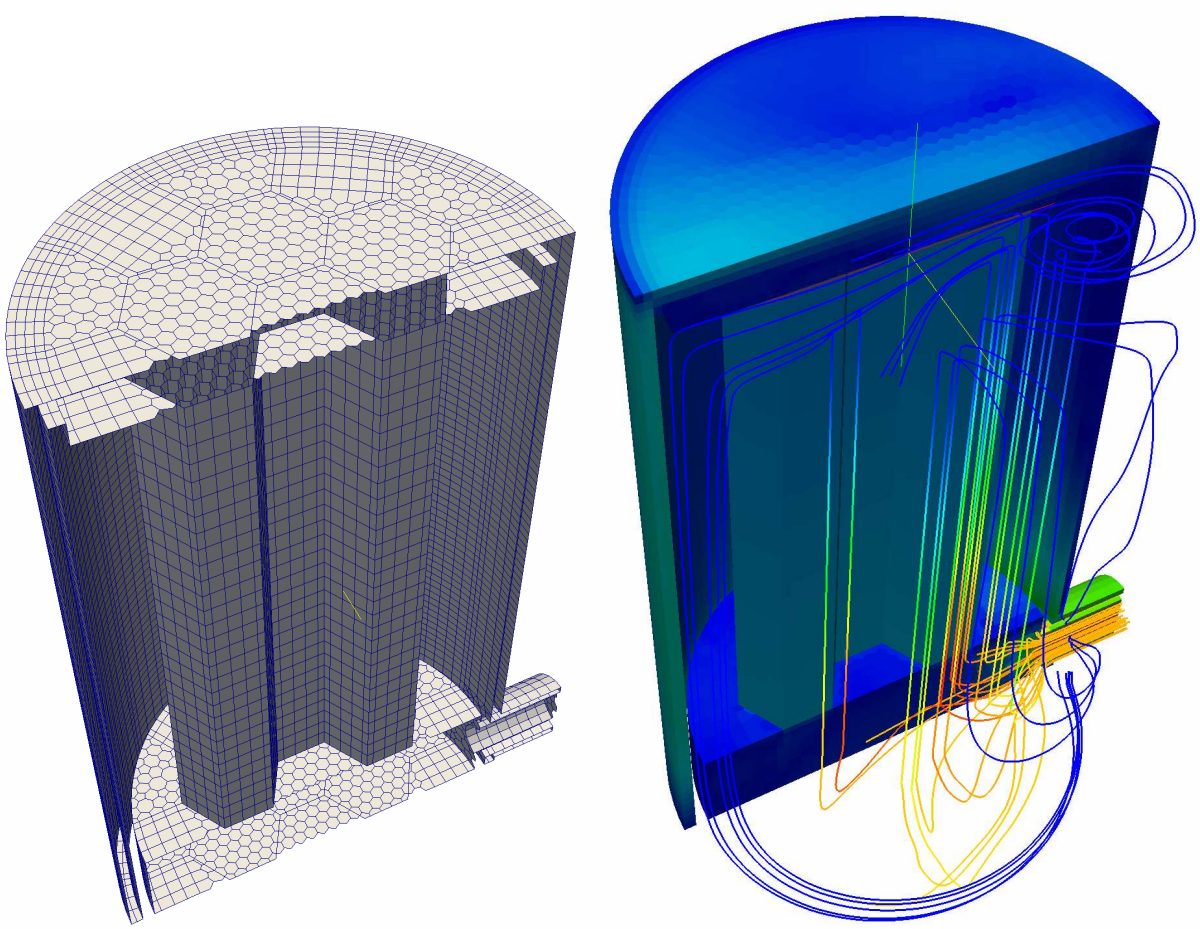

(a) (b)

Figure 6. Coarse Mesh CFD (a) Mesh and (b) Solution for a Small Representative Prismatic HTR

7. CONCLUSIONS

We have introduced a coarse and fine mesh CFD solution scheme applicable for multi-scale CFD simulation of VHTRs. A consistent set of conservation equations for a two-phase mixture of gas and stationary solid have been selected and suitable assumptions made to ensure the equations reduce to the single phase conservation equations for the case where void fraction is unity. An unstructured Finite Volume discretisation was chosen using a semi-implicit PISO-style pressure velocity coupling. The discretisation of the conservation equations uses a new pressure interpolation scheme capable of capturing the discontinuity in pressure across relatively large changes in void fraction.

A test solver supporting fully unstructured three-dimensional time-dependent compressible flows, including buoyancy effects, with a variable porosity field was implemented using the

OpenFOAM multiphysics toolkit. The solver is stable for one-, two- and three-dimensional problems within the typical Courant number limit of 0.3. Initial test calculations suggest that the solver is capable of capturing sharp discontinuities in void fraction, although small inconsistencies are noted for flows with extreme changes in void fraction where compressibility effects are important. These inconsistencies may be treated by smoothing the change in void fraction over more than one cell length. This remedy, however, is not ideal and further work should be carried out to resolve this issue. The pressure interpolation scheme performs well in general, however is incapable of capturing strong flow discontinuities such as shock waves. For these flows, the scheme is unbounded, resulting in unstable solutions. This is likely related to the inconsistencies noted for extreme changes in void fraction.

For typical VHTR flow phenomena the new solver shows promise as an effective candidate for predicting the flow behavior on multiple scales, as it is capable of modeling both fine mesh single phase flows as well as coarse mesh flows in homogenized regions containing both fluid and solid materials.

7.1. Future Work

Future work is recommended in the following areas:

- Additional work is required to address the unbounded behavior of the pressure interpolation scheme to certain flows, as well as the inconsistencies noted near extreme changes in void fraction. These two issues are likely related.
- The accuracy of coarse mesh solutions is largely dependent on the accuracy of the homogenized parameters supplied to the calculation. Future work will focus on generating suitable homogenized fluid flow and heat transfer parameters based on fine-scale solution using a consistent methodology. This will open up the possibility for the development of a hierarchical multi-scale solution scheme for this reactor type.
- The fluid flow calculation will be coupled to a solid material heat transfer calculation in the future. This coupling will include heat transfer at solid surfaces as well as the heat transfer between the fluid and solid phases present in homogenized regions.

ACKNOWLEDGEMENTS

We would like to acknowledge and thank the Very High Temperature Reactor Technology Development Office of the Idaho National Laboratories for their funding and support of this work.

REFERENCES

1. S. Struth, *THERMIX-DIREKT: ein Rechenprogramm zur instationaeren, zweidimensionale Simulation thermohydraulischer Transienten*, ISR-KFA Jülich, August (1994)
2. H. Gerwin, W. Scherer and E. Teuchert, “The TINTE Modular Code System for computational simulation of transient processes in the primary circuit of a pebble-bed high-temperature gas-cooled reactor,” *Nuclear Science and Engineering*, **Volume 103**, pp.302–312 (1989)

3. H. Park, D. Knoll, H. Sato and W. Taitano, *Progress on PRONGHORN application to NGNP related problems*, Idaho National Laboratories (INL), August (2009)
4. O. Cioni, M. Marchand, G. Geffraye and F. Ducros, "3D thermal-hydraulic calculations of a modular block-type HTR core," *Nuclear Engineering and Design*, **Volume 236**, pp.565–573 (2006)
5. W. D. Pointer and J. W. Thomas, "Steady-state, whole-core prismatic VHTR simulation including core bypass," *Proceedings of ICAPP '10*, San Diego, CA, USA, June 13-17 (2010)
6. R. Saurel and R. Abgrall, "A Multiphase Godunov Method for Compressible Multifluid and Multiphase Flows," *Journal of Computational Physics*, **Volume 150**, Issue 2, pp.425-467 (1999)
7. R. Saurel and O. Lemetayer, "A multiphase model for compressible flows with interfaces, shocks, detonation waves and cavitation," *Journal of Fluid Mechanics*, **Volume 431**, pp.239-271 (2001)
8. M.H.J. Pedras and M.J.S. de Lemos, "Macroscopic turbulence modeling for incompressible flow through undeformable porous media," *International Journal of Heat and Mass Transfer*, **Volume 44**, pp.1081-1093 (2001)
9. M. Chandesris, G. Serre and P. Sagaut, "A macroscopic turbulence model for flow in porous media suited for channel, pipe and rod bundle flows," *International Journal of Heat and Mass Transfer*, **Volume 49**, pp.2739–2750 (2006)
10. R.I. Issa, "Solution of the Implicitly Discretized Fluid Flow Equation by Operator Splitting," *Journal of Computational Physics*, **Volume 62**, pp.49–65 (1986)
11. P. du Toit, *Konvek, Direkt, TINTE, OpenFOAM, An Investigation into Different Discretization Techniques Suitable for Lumped Parameter Fluid Flow Numerical Methods*, Revision A, Draft document, PBMR Pty. Ltd. (2009)
12. H. Jasak, *Error Analysis and Estimation for the Finite Volume Method with Applications to Fluid Flows*, PhD. Thesis, Imperial College, University of London (1996)
13. H. G. Weller, G. Tabor, H. Jasak and C. Fureby, "A tensorial approach to computational continuum mechanics using object-oriented techniques," *Computers in Physics*, **Volume 12**, Issue 6, pp.620-631, November (1998)